

Optical Transmission Enhancement of Ionic Crystals via Superionic Fluoride Transfer: Growing VUV-Transparent Radioactive Crystals

Kjeld Beeks,¹ Tomas Sikorsky,¹ Fabian Schaden,¹ Martin Pressler,¹ Felix Schneider,¹ Björn N. Koch,² Thomas Pronebner,¹ David Werban,¹ Niyusha Hosseini,¹ Georgy Kazakov,¹ Jan Welch,³ Johannes H. Sterba,³ Florian Kraus,² and Thorsten Schumm¹

¹*Institute for Atomic and Subatomic Physics, TU Wien, Stadionallee 2, 1020, Vienna, Austria*

²*Anorganische Chemie, Fluorchemie, Fachbereich Chemie,*

Phillips-Universität Marburg, Hans-Meerwein-Str. 4, 35032 Marburg

³*CLIP, TRIGA Center Atominstytut, TU Wien, Stadionallee 2, 1020, Vienna, Austria*

(Dated: March 4, 2024)

The 8 eV first nuclear excited state in ^{229}Th is a candidate for implementing a nuclear clock. Doping ^{229}Th into ionic crystals such as CaF_2 is expected to suppress non-radiative decay, enabling nuclear spectroscopy and the realization of a solid-state optical clock. Yet, the inherent radioactivity of ^{229}Th prohibits the growth of high-quality single crystals with high ^{229}Th concentration; radiolysis causes fluoride loss, increasing absorption at 8 eV. These radioactively doped crystals are thus a unique material for which a deeper analysis of the physical effects of radioactivity on growth, crystal structure and electronic properties is presented. Following the analysis, we overcome the increase in absorption at 8 eV by annealing ^{229}Th doped CaF_2 at 1250 °C in CF_4 . This technique allows to adjust the fluoride content without crystal melting, preserving its single-crystal structure. Superionic state annealing ensures rapid fluoride distribution, creating fully transparent and radiation-hard crystals. This approach enables control over the charge state of dopants which can be used in deep UV optics, laser crystals, scintillators, and nuclear clocks.

Thorium-229 (^{229}Th), possessing an 8 eV and approximately 600-second lifetime first nuclear excited state (isomer state), enables high-precision vacuum ultraviolet (VUV) laser spectroscopy [1–3]. The anomalously low energy of this excited state offers the potential for the construction of an optical clock based on a nuclear transition [4, 5]. The structure of the nuclear levels is governed by both Coulomb and nuclear forces [6]. This allows probing of these forces via nuclear spectroscopy, paving the way for new fundamental research: For example the search for dark matter, or potential drifts in the fine-structure constant [7, 8].

^{229}Th is required to be in a 3+ or higher charge state to suppress the non-radiative decay [9]. The possibility of trapping charged ^{229}Th in a solid-state matrix offers an alternative to ion traps. In the solid, the nucleus is isolated due to the small interaction with its chemical environment [10]. Ionic crystals such as CaF_2 are an excellent choice as host material for the ^{229}Th based nuclear clock [11]. The ionic character of these crystals naturally forces the ^{229}Th into a 4+ charged state, substituting the calcium (Ca^{2+}) cation [12, 13], and their large band gaps make them transparent to wavelengths around 150 nm or 8 eV [14]. Ionic crystals such as oxides and fluorides display good scintillator properties and are resistant to VUV radiation, making them suitable to host the radioactive ^{229}Th and observe its radiative decay [2, 15]. In this experiment, calcium fluoride (CaF_2) was chosen as the host material due to its excellent scintillator properties [16], simple cubic structure [17], large 12 eV electronic and 10 eV optical bandgap [14], and an unchanged 10 eV optical bandgap after thorium [18] doping. Both ^{232}Th and

^{229}Th were used to grow single crystalline $\text{Th}:\text{CaF}_2$ using the vertical gradient freeze method [19].

The process of growing CaF_2 in a vacuum environment leads to a fluoride ion (F^-) deficit due to thermal dissociation of CaF_2 and its reaction with the residual water in the system [22, 23]. This sequence leads to the formation of a non-stoichiometric or fluoride-deficient crystal. To counterbalance the loss in fluoride ions, the crystal tends to generate metallic Ca nanoparticles [18], which possess the capacity to absorb and scatter light [24], especially within the VUV and optical range. Non-stoichiometry in all ionic crystals leads to changes in the configuration: either change of charge state of cations or formation of metal colloids [25]. Although this variation in configuration has been thoroughly examined in oxides like CeO_2 [26, 27], it has not been extensively studied for fluorides and there is a lack of common terminology, understanding and means of controlling the compositions [28–32].

Due to the presence of a radioactive element during growth, radiolysis causes enhanced dissociation of CaF_2 [19, 33]. The strong dissociation creates a very non-stoichiometric composition. The change in composition leads to a change of dopant configuration and absorption profile, as was first observed in the work of Cirillo et al. (1987) [28]. Here, adding F_2 to $\text{Eu}^{2+}:\text{CaF}_2$ changed the charge state of Eu and thus the absorption profile of the crystal. A lack of fluoride in the crystal is compensated for by reducing the calcium to neutral, and the dopant to a lower charge state. By adding fluoride the charge state of the dopant can be increased and the calcium oxidized.

Radioactivity not only affects growth: (doped) CaF_2

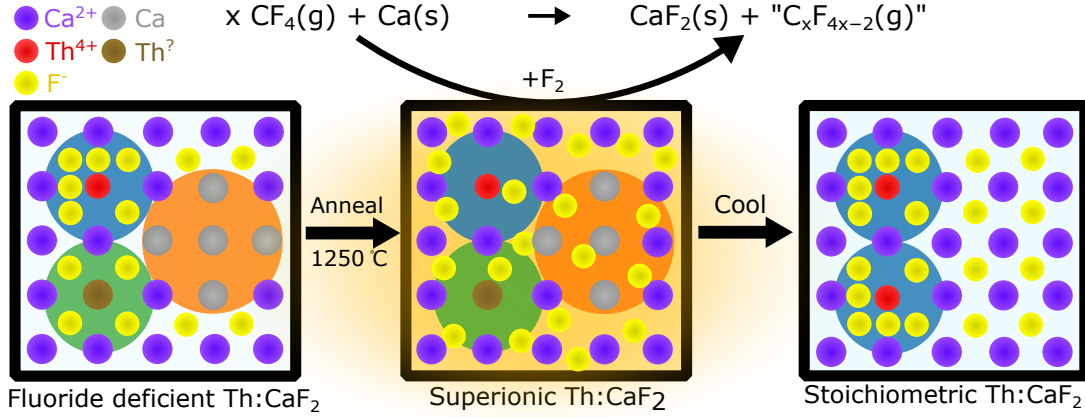


FIG. 1. Schematic representation of the fluorination cycle and the corresponding change in local crystal structure. The fluoride deficient, imperfect crystal shows Ca metallic nanoparticles (orange region, right), Th doping with unknown surrounding and charge state (green region, bottom left), and Th stoichiometrically surrounded by fluoride ions (blue region, top left) [20]. The associated absorption peaks are identified in the text and measured in Figure 3. Adding F atoms at superionic temperatures distributes the anions quickly through the crystal due to the increased mobility [21]. After slowly cooling down, the crystal reaches a stoichiometric composition with the dopant in the ideal surrounding. The increase in blue absorption and decrease in all others is shown in Figure 4.

subjected to radiation from radioactive decay after growth shows complex behavior centered around fluoride motion in the lattice [34]. The $^{229}\text{Th}:\text{CaF}_2$ crystals therefore are a unique and complex system for which we give a concise description, following the literature [18, 24, 35–37].

The presence of a radioactive element in the CaF_2 matrix is a source of excitation of the lattice, which produces defects and aggregates which lie at the core of understanding the dynamic processes. Mainly the motion of fluorine determines the produced defects and their respective absorption and emission bands: fluoride moves through the crystal expending much less energy (0.6–1.5 eV) than the calcium ions and the formation energy of an anion Frenkel pair (F^- interstitial and vacancy) is 2.7 eV as compared to 6 eV to form a cation Frenkel pair. Therefore the main defects in CaF_2 are related to fluoride: F, H and V_k centers. The F center is an electron trapped at the location of a fluoride vacancy, which is similar to an electron in a box. Therefore the F center has rich optical absorption and emission bands. Th H center is a fluoride interstitial, which shares a trapped hole with a lattice fluoride thereby creating an F_2^- dimer with high mobility. The V_k center is a trapped hole shared between two lattice fluorides, thereby also creating an F_2^- dimer.

The energy deposited by ^{229}Th and its daughters through α and β decay is in the range of 100 keV to 8.5 MeV per decay. Such a high energy excitation will produce core shell holes and highly excited electrons. These will decay through various mechanisms such as Auger electrons, x-ray emission and plasmons to electron hole pairs (12.2 eV formation energy), and self-trapped-excitons (STE, formation energy 11.18 eV, absorption

bands at 282 and 482 nm, emission bands from 200 to 500 nm). The electron hole pair can annihilate under photon emission, non-radiatively create a separate F and H center in the lattice (imperfect damaged crystal) or decay to a STE. The STE initially constitutes of a self-trapped-hole (V_k center) and a captured electron, but quickly decays to an F and H pair. The F-H pair again either annihilates and emits a photon, or decays non-radiatively and leaves a separate F and H center in the crystal.

The F center (absorption at 378 nm, emission at 585 nm) agglomerates into higher order M (2 F), R (3 F) and N (4 F) centers and continues to form Ca metallic colloids (fluoride vacancy agglomeration in CaF_2 is metallic Ca) as it is energetically favorable. The agglomeration shifts absorption and emission bands to lower energies. Most importantly the Ca colloids absorb in two bands, from 550 to 960 nm and 160 to 200 nm depending on their size [32]. In thorium doped crystals these colloids absorb around 150 nm [18] due to the change in refractive index.

The H center (absorption at 310 nm) can further collapse either to an impurity trapped hole (identified at 295 nm for Th) or two H centers form an interstitial dimer (two interstitial F^- that share a hole, F_2^-). The dimer formation can also aggregate to form dislocation loops (as observed). Through hopping, the single (or higher order) F and H centers can again find one another and annihilate (evaporate) under photon emission, thereby again producing a perfect crystal. If a stoichiometric amount of Ca and F_2 is present, this can be done through annealing at 600 °C. If not, fluoride annealing needs to be applied.

Due to the constant internal irradiation of this crystal, the above processes are dynamic and the fluorides are in motion. Defects will accumulate until a steady state of growth and evaporation of Ca colloids and H center dimers is reached. The constant irradiation also provides a constant stream of Cherenkov photons (200 to 122 nm). Irradiated non-stoichiometric CaF_2 damages faster, as a larger amount of F and H centers is already present to compensate for non-stoichiometry, which can quickly aggregate upon irradiation to larger more absorbing defects. The damage steady state is reached quicker and annealing does not completely repair radiation damage. To create more transparent and radiation resistant CaF_2 , fluorine needs to be added for a stoichiometric crystal.

Therefore we study the impact of the $\text{Th}:\text{CaF}_2$ crystal composition on its VUV transmission and the electronic structure of the dopant sites. Due to the ^{229}Th radioactivity, radiolysis becomes the major cause of the fluorine (F_2) loss during the growth phase. This substantial F_2 loss modifies the electronic structure of the CaF_2 crystal, resulting in a consequential change in its absorption profile [19]. The large resulting VUV absorption would make such a $^{229}\text{Th}:\text{CaF}_2$ unsuitable for a nuclear optical clock.

We follow [28] and developed a novel and safer experimental method that does not require toxic F_2 gas to add fluoride ions to already grown, single-crystalline, Th doped CaF_2 and still dramatically improve the transmission profile.

We use an induction heated carbon crucible to anneal $\text{Th}:\text{CaF}_2$ at above its superionic temperature, but below its melting temperature, in a carbon tetrafluoride (CF_4) atmosphere. The crystal is placed in the center of an induction coil in a carbon crucible, after which the system is evacuated to approximately 1×10^{-6} mbar. The chamber is then filled with 1.1 bar CF_4 . In the heating step, the carbon crucible is heated using the induction coil (1300 °C, heating rate 20 K/min) while the walls of the vacuum system are water-cooled, creating a steep temperature gradient. The temperature gradient causes the CF_4 gas to be reactive only at the crystal surface and inert at the vacuum system walls, which significantly reduces safety concerns while ensuring the efficiency of the process. After annealing for 1 hour while holding the temperature, the system is cooled down (cooling rate 1 K/min) and at room temperature the CF_4 is replaced by N_2 . A schematic representation of the process is shown in Figure 1.

Above the superionic transition temperature of CaF_2 (1250 °C [21]), but below the melting temperature, fluoride anions exhibit high mobility while calcium cations remain immobile. The mobility of fluoride ions ensures their uniform distribution throughout the bulk crystal.

To produce a heavily fluoride deficient crystal, we first performed superionic annealing in vacuum instead of a CF_4 atmosphere on a $^{232}\text{Th}:\text{CaF}_2$ crystal. Excessive flu-

orine loss from the crystal during vacuum superionic annealing for 24 hours has turned an initially transparent crystal into a cloudy and opaque one (see Figure 2, left). Annealing in an argon atmosphere was also performed, producing a similar but less deficient crystal. The formation of calcium metal colloids can explain the opacity [24]. In the following phase, which consists of CF_4 annealing in two cycles of one hour each, the crystal regains its visible transparency (see Figure 2, middle and right).

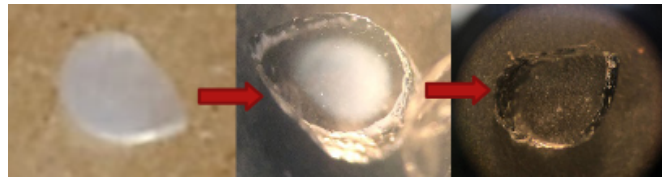


FIG. 2. Annealing of a fluoride-deficient $^{232}\text{Th}:\text{CaF}_2$ crystal in two steps, each step lasting one hour. Ca colloids absorb and scatter heavily in the visible region [24]. It is clearly seen that after the first cycle the opacity recedes to the center, while after the second fluorination step the crystal has fully regained optical transmission.

Following the fluorination treatment, we observed a significant improvement in the VUV transparency of the $^{229}\text{Th}:\text{CaF}_2$ crystals, as shown in Figure 3. Note that this crystal was fully opaque around 8 eV (150 nm) and hence unusable for nuclear laser spectroscopy directly after growth. After several cycles, the absorption was lower as compared to the non-radioactive ^{232}Th doped crystal, indicating CF_4 could improve its absorption profile as well (as was done in [13]). When comparing this absorption spectrum to pure CaF_2 , three absorption centers can be seen to appear and disappear. The absorption spectrum was recorded using a McPherson 204/302 VUV spectrometer, as described in the work of Beeks et al. [18]. As verified by gamma spectroscopy, the annealing process did not cause any quantifiable loss of radioactivity, indicating no noticeable reduction of the ^{229}Th concentration.

To quantitatively describe the VUV absorption profile over the time of fluorination, we identify three absorption lines (assuming gaussian profile) in Figure 3. We attribute the 122 nm absorption to the Th^{4+} charge transfer state [38, 39], the 130 nm absorption to Th ions in a different surrounding, and the broad 150 nm absorption to Ca metallic colloids [24, 40]. The 130 nm absorption is likely caused by a change in the surrounding of the Th ion: either the change of charge state of the Th atom to neutral/1+/2+/3+ due to the fluoride deficiency, reaction of the non-stoichiometric CaF_2 with oxygen in the air thereby replacing the F atoms surrounding Th by O atoms or a change in charge compensation mechanism to for example a Ca vacancy [12, 13]. Investigations of the 130 nm absorption line are ongoing. In Figure 4 it can be seen that in low and high-doped crystals the 122 nm

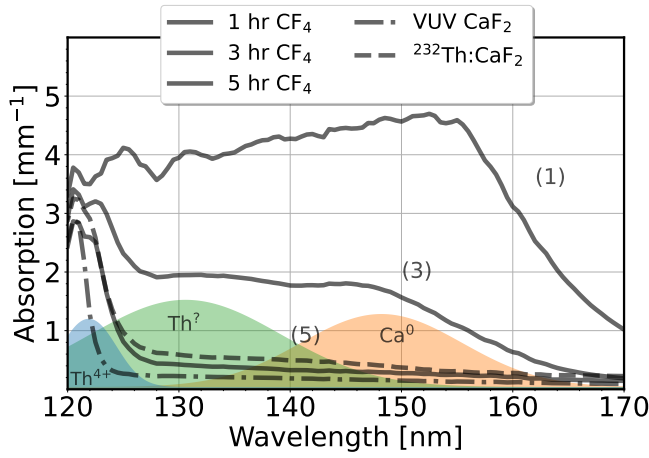


FIG. 3. VUV absorption spectrum of a $6 \times 10^{18} \text{ cm}^{-3}$ doped $^{229}\text{Th}:\text{CaF}_2$ crystal for different superionic fluoride annealing durations (numbers indicate annealing time). To compare, absorption of a $^{232}\text{Th}:\text{CaF}_2$ crystal with similar doping concentration without fluoride annealing is plotted and that of a VUV grade pure CaF_2 sample. The three absorption line centers shown in Figure 1 are fitted with gaussian functions, while compensating for the undoped CaF_2 absorption background and drawn in the figure with the same colors and indicated defect.

absorption increases with cycle number, indicating an increase in Th^{4+} with fully charge-compensated surrounding. The other two absorption lines assigned to Ca colloids and Th in a different surrounding both diminish. Effectively the electronic structure of the Th dopants is manipulated by adding fluoride ions to the deficient crystal.

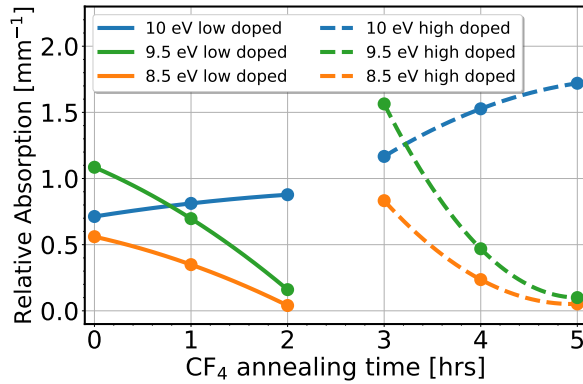


FIG. 4. Intensities of the three absorption lines relative to undoped CaF_2 identified in Figure 1 and Figure 3 at 121.9 nm, 130.5 nm and 148.2 nm or approximately 10 eV, 9.5 eV and 8.5 eV is plotted as a function of superionic fluoride transfer time for two $^{229}\text{Th}:\text{CaF}_2$ crystals (1×10^{18} and $6 \times 10^{18} \text{ cm}^{-3}$). Data points are connected with splines to lead the eye.

After fluorination of the $^{229}\text{Th}:\text{CaF}_2$, no change in color is observed in the crystal over the course of a year as opposed to the original fluoride deficient crystals [19].

The VUV transmission decreased from 50% to 35% over the course of 1 year, as opposed to complete VUV opacity in 3 days for non-fluorinated crystals. The original transmission could be completely regained through superionic fluoride transfer. After a year, no other changes in the radioactive crystals are observed such as cracking, thus it is concluded the radiation hardness significantly increased after fluorination as predicted.

Alternative methods of fluorination of low-doped $^{229}\text{Th}:\text{CaF}_2$ crystals were also tested. Highly fluoride deficient crystals (opaque) were treated using 3 different methods.

The first method was annealing in an F_2 atmosphere. A Mg sample holder was passivated for two days at 600°C (heating rate: 4 K h^{-1} , cooling rate: 1 K min^{-1}) in an F_2 flow (20% F_2 in N_2 atmosphere, $5 \text{ cm}^3 \text{ min}^{-1}$). The $^{229}\text{Th}:\text{CaF}_2$ crystal was placed in the sample holder and was fluorinated for five days at 600°C (heating rate: 4 K h^{-1} , cooling rate: 1 K min^{-1}) in an F_2 flow (20% F_2 in N_2 atmosphere, $5 \text{ cm}^3 \text{ min}^{-1}$).

The second method was treatment using an NF_3 plasma. In this method a Ni sample holder was passivated in a fluorine plasma at room temperature for one hour. The $^{229}\text{Th}:\text{CaF}_2$ crystal was placed in the sample holder and was fluorinated in a fluorine plasma at room temperature for three hours. NF_3 was used as feeding gas with a flow rate of $30 \text{ cm}^3 \text{ min}^{-1}$.

The third method was treatment in a F_2 filled autoclave. In this method a Ni sample holder was passivated for one day at 400°C and approximately 400 bar (heating rate: 100 K h^{-1} , cooling rate: 4 K min^{-1} , 20% F_2 in Ar atmosphere). The $^{229}\text{Th}:\text{CaF}_2$ crystal was placed in the Ni sample holder and was high-pressure fluorinated at 400°C and approximately 400 bar for five days (heating rate: 100 K h^{-1} , cooling rate: 4 K min^{-1} , 50% F_2 in Ar atmosphere).

The resulting crystals still displayed high absorption as can be seen in Figure 5. The 5 days of F_2 annealing at 600°C displayed results similar to 1 hour of CF_4 annealing at 1250°C .

Compared to alternative treatments, only superionic annealing under CF_4 atmosphere demonstrated a significant improvement in the VUV transmission (compare Figure 3 with Figure 5). Consequently, it can be concluded that the superionic state of CaF_2 allows for efficient and rapid homogeneous distribution of the acquired fluoride ions. This contrasts with other methods where the solid phase of the crystal prevents fluoride ion diffusion through the crystal.

Many facts have been gathered on $^{229}\text{Th}:\text{CaF}_2$: The observed absorption centers at 122, 130 and 150 nm, their change with fluoride content and the known fluorescence of $^{229}\text{Th}:\text{CaF}_2$ at 184 nm [2] (and at 168, 230, 238, 250 and 295 nm [18]). Aside from the 150 nm absorption which has been identified as Ca nanoparticles [24], we can speculate on the origin of the other absorption and

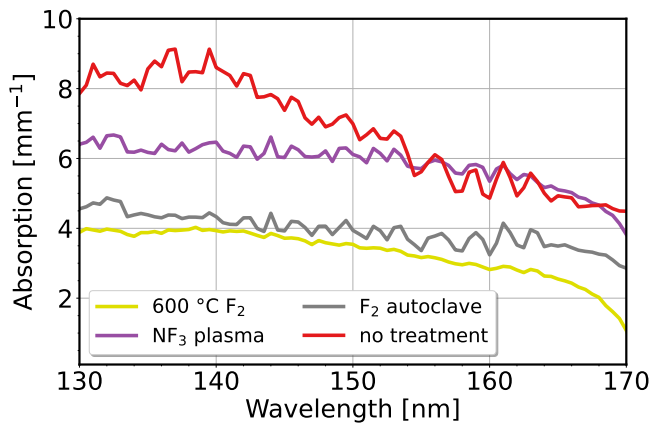


FIG. 5. Absorption spectra of different segments of a $1 \times 10^{-17} \text{ cm}^{-3}$ doped $^{229}\text{Th}:\text{CaF}_2$ crystal that was grown using 1 MBq of activity for different fluoride treatments. No reliable data could be obtained below 130 nm due to the high absorption.

fluorescence bands. We will compare thorium with chemical analogues such as cerium and hafnium.

The cerium analogue we will use to compare spectroscopic data in CaF_2 , as its 4+ and more common 3+ states have similar electronic configuration. Due to relativistic effects, the differences between Ce and Th might be large. The hafnium analogue we will use for the charge state thorium assumes, as neutral hafnium has a similar valence electron configuration ($5d^2 6s^2$ vs. $6d^2 7s^2$) and chemically behaves similar to thorium. Just as thorium, hafnium almost exclusively takes a 4+ charge state, as opposed to cerium.

It is known that the rare earths in CaF_2 reduce upon X-ray irradiation [41]. Hf^{4+} doped in YPO_4 can be reduced to Hf^{3+} by X-ray irradiation [42] and it is known that the actinides reduce through self-irradiation in CaF_2 [43]. We thus speculate that thorium undergoes the same process from 4+ to 3+. As F centers and electrons in the conduction band are constantly produced, the Th^{4+} cations will attract them through the coulomb force more strongly compared to Ca^{2+} cations. Through the change of absorption intensities with fluoride annealing we assert that the change in charge state is not only through irradiation but also stoichiometry. It can be argued that these are the same processes: Locally, the creation of F centers through irradiation creates non-stoichiometry thereby changing the charge state of the dopant.

Comparing Th^{3+} to Ce^{3+} doped in CaF_2 , we can find that Ce^{3+} has several $4f^n$ to $4f^{n-1}5d$ excitations around 180 nm [44, 45]. The bare Th^{3+} ion has a strong $6d$ to $7p$ line at 170 nm [46]. Fluorescence lines in the VUV are known to exist for 3+ heavy rare earth ions in CaF_2 [47]. We speculate that the fluoride deficient CaF_2 contains some Th^{3+} , that is optically active through absorption at 130 nm and emission at 168 and 180 nm. Through

addition of fluoride these disappear and only the Th^{4+} absorption at 120 nm remains. This charge transfer state was predicted [38, 39] and would constitute creating an electron hole pair on the thorium dopant and a neighboring fluoride. We speculate that this pair decays to a defect stabilized V_k plus electron center [48], which emits at 295 nm [18].

This report demonstrates the enhancement of optical transmission in ionic crystals through superionic fluoride transfer. This superionic state substantially decreases the treatment duration. Furthermore, our findings suggest the possibility of controlling the dopant surrounding in CaF_2 by the addition or removal of F^- , although the removal process carries a potential risk of creating Ca metallic nanoparticles. We have developed a simple and safe method of fluorine manipulation in fluoride ionic crystals. Utilizing this method, we are able to fabricate highly transparent, heavily doped $^{229}\text{Th}:\text{CaF}_2$ crystals for a solid-state nuclear clock. The manipulation of the electronic structure brings the potential for advancements in optics, scintillator and laser crystal development by optimizing light absorption and emission through dopant and cation surrounding control (e.g., $\text{Eu}:\text{CaF}_2$).

Acknowledgements

This work is part of the thorium nuclear clock project that has received funding from the European Research Council (ERC) under the European Union's Horizon 2020 research and innovation programme (Grant Agreement No. 856415). The research was supported by the Austrian Science Fund (FWF) Projects: I5971 (REThorIC) and P 33627 (NQRclock).

-
- [1] B. Seiferle, L. von der Wense, P. V. Bilous, I. Amersdorfer, C. Lemell, F. Libisch, S. Stellmer, T. Schumm, C. E. Düllmann, A. Pálffy, and P. G. Thirolf, *Nature* **573**, 243 (2019).
 - [2] S. Kraemer, J. Moens, M. Athanasakis-Kaklamanakis, S. Bara, K. Beeks, P. Chhetri, K. Chrysalidis, A. Claessens, T. E. Cocolios, J. G. Correia, *et al.*, *Nature* **617**, 706 (2023).
 - [3] T. Masuda, A. Yoshimi, A. Fujieda, H. Fujimoto, H. Haba, H. Hara, T. Hiraki, H. Kaino, Y. Kasamatsu, S. Kitao, K. Konashi, Y. Miyamoto, K. Okai, S. Okubo, N. Sasao, M. Seto, T. Schumm, Y. Shigekawa, K. Suzuki, S. Stellmer, K. Tamasaku, S. Uetake, M. Watanabe, T. Watanabe, Y. Yasuda, A. Yamaguchi, Y. Yoda, T. Yokokita, M. Yoshimura, and K. Yoshimura, *Nature* **573**, 238 (2019).
 - [4] E. Peik and C. Tamm, *Europhysics Letters* **61**, 181 (2003).
 - [5] K. Beeks, T. Sikorsky, T. Schumm, J. Thielking, M. V.

- Okhupkin, and E. Peik, *Nature Reviews Physics*, 1 (2021).
- [6] A. Hayes and J. Friar, *Physics Letters B* **650**, 229 (2007).
- [7] E. Peik, T. Schumm, M. S. Safronova, A. Pálffy, J. Weitenberg, and P. G. Thirolf, *Quantum Science and Technology* **6**, 034002 (2021).
- [8] P. Fadeev, J. C. Berengut, and V. V. Flambaum, *Phys. Rev. A* **102**, 052833 (2020).
- [9] E. Peik and M. Okhupkin, *Comptes Rendus Physique*, *Comptes Rendus Physique* **16**, 516 (2015), [arXiv:1502.07322v1](#).
- [10] G. A. Kazakov, A. N. Litvinov, V. I. Romanenko, L. P. Yatsenko, A. V. Romanenko, M. Schreitzl, G. Winkler, and T. Schumm, *New Journal of Physics* **14**, 083019 (2012).
- [11] M. P. Hehlen, R. R. Greco, W. G. Rellergert, S. T. Sullivan, D. DeMille, R. A. Jackson, E. R. Hudson, and J. R. Torgerson, *Journal of Luminescence* **133**, 91 (2013), 16th International Conference on Luminescence ICL'11.
- [12] M. Pimon, A. Grüneis, P. Mohn, and T. Schumm, *Crystals* **12**, 1128 (2022).
- [13] Q. Gong, S. Tao, C. Zhao, Y. Hang, S. Zhu, and L. Ma, *Inorganic Chemistry* (2024).
- [14] G. W. Rubloff, *Physical review B* **5**, 662 (1972).
- [15] T. YANAGIDA, *Proceedings of the Japan Academy, Series B* **94**, 75 (2018).
- [16] P. A. Rodnyi, *Physical processes in inorganic scintillators*, Vol. 14 (CRC press, 1997).
- [17] “CaF₂ crystal structure: Datasheet from “pauling file multinationals edition – 2012” in *springermaterials*,” Copyright 2016 Springer-Verlag Berlin Heidelberg & Material Phases Data System (MPDS), Switzerland & National Institute for Materials Science (NIMS), Japan.
- [18] K. Beeks and T. Schumm, *The Nuclear Excitation of Thorium-229 in the CaF₂ Environment*, Ph.D. thesis, Wien (2022).
- [19] K. Beeks, T. Sikorsky, V. Rosecker, M. Pressler, F. Schaden, D. Werban, N. Hosseini, L. Rudischer, F. Schneider, P. Berwian, *et al.*, *Scientific Reports* **13**, 3897 (2023).
- [20] P. Dessovic, P. Mohn, R. Jackson, G. Winkler, M. Schreitzl, G. Kazakov, and T. Schumm, *Journal of Physics: Condensed Matter* **26**, 105402 (2014).
- [21] M. Gillan, *Journal of Physics C: Solid State Physics* **19**, 3391 (1986).
- [22] K. Recker and R. Leckebusch, *Journal of Crystal Growth* **9**, 274 (1971).
- [23] W. Bollmann, *physica status solidi (a)* **57**, 601 (1980).
- [24] S. Rix, *Radiation-induced defects in calcium fluoride and their influence on material properties under 193 nm laser irradiation*, Ph.D. thesis, Mainz, Univ., Diss., 2011 (2011).
- [25] A. Hughes and S. Jain, *Advances in Physics* **28**, 717 (1979).
- [26] Q. Li, L. Song, Z. Liang, M. Sun, T. Wu, B. Huang, F. Luo, Y. Du, and C.-H. Yan, *Advanced Energy and Sustainability Research* **2**, 2000063 (2021).
- [27] C. Barth, C. Laffon, R. Olbrich, A. Ranguis, P. Parent, and M. Reichling, *Scientific Reports* **6**, 21165 (2016).
- [28] K. M. Cirillo and J. C. Wright, *Journal of crystal growth* **85**, 453 (1987).
- [29] M. Dubois, B. Dieudonne, A. Mesbah, P. Bonnet, M. El-Ghoozi, G. Renaudin, and D. Avignant, *Journal of Solid State Chemistry* **184**, 220 (2011).
- [30] F. Wang, X. Fan, D. Pi, and M. Wang, *Solid state communications* **133**, 775 (2005).
- [31] O. Antonyak, Z. Khapko, and M. Chylii, *Radiation Effects and Defects in Solids* **172**, 456 (2017).
- [32] A. E. Angervaks, A. V. Veniaminov, M. V. Stolyarchuk, V. E. Vasilev, I. Kudryavtseva, P. P. Fedorov, and A. I. Ryskin, *J. Opt. Soc. Am. B* **35**, 1288 (2018).
- [33] J. Schmedt auf der Günne, M. Mangstl, and F. Kraus, *Angewandte Chemie International Edition* **51**, 7847 (2012).
- [34] V. R. Celinski, M. Ditter, F. Kraus, F. Fujara, and J. Schmedt auf der Günne, *Chemistry—A European Journal* **22**, 18388 (2016).
- [35] W. Hayes and A. M. Stoneham, *Defects and defect processes in nonmetallic solids* (Courier Corporation, 2012).
- [36] C. Catlow, K. Diller, and L. Hobbs, *Philosophical Magazine A* **42**, 123 (1980).
- [37] P. A. Rodnyi, *Physical processes in inorganic scintillators* (CRC press, 2020).
- [38] B. S. Nickerson, M. Pimon, P. V. Bilous, J. Gugler, K. Beeks, T. Sikorsky, P. Mohn, T. Schumm, and A. Pálffy, *Phys. Rev. Lett.* **125**, 032501 (2020).
- [39] B. S. Nickerson, M. Pimon, P. V. Bilous, J. Gugler, G. A. Kazakov, T. Sikorsky, K. Beeks, A. Grüneis, T. Schumm, and A. Pálffy, *Physical Review A* **103**, 053120 (2021).
- [40] A. I. Ryskin, P. P. Fedorov, N. T. Bagraev, A. Lushchik, E. Vasil’chenko, A. E. Angervaks, and I. Kudryavtseva, *Journal of Fluorine Chemistry* **200**, 109 (2017).
- [41] Z. Kiss and D. Staebler, *Physical Review Letters* **14**, 691 (1965).
- [42] V. Laguta, M. Buryi, M. Nikl, J. Zeler, E. Zych, and M. Bettinelli, *Journal of Materials Chemistry C* **7**, 11473 (2019).
- [43] J. Stacy, N. Edelstein, and R. McLaughlin, *The Journal of Chemical Physics* **57**, 4980 (1972).
- [44] L. Van Pieterson, M. Reid, R. Wegh, S. Soverna, and A. Meijerink, *Physical Review B* **65**, 045113 (2002).
- [45] M. Yamaga, S. Yabashi, Y. Masui, M. Honda, H. Takahashi, M. Sakai, N. Sarukura, J.-P. Wells, and G. Jones, *Journal of luminescence* **108**, 307 (2004).
- [46] P. Klinkenberg and R. Lang, *Physica* **15**, 774 (1949).
- [47] L. Van Pieterson, M. Reid, G. Burdick, and A. Meijerink, *Physical Review B* **65**, 045114 (2002).
- [48] J. Beaumont, W. Hayes, D. Kirk, and G. Summers, *Proceedings of the Royal Society of London. A. Mathematical and Physical Sciences* **315**, 69 (1970).